Shot noise spectroscopy on a semiconductor quantum dot in the elastic and inelastic cotunneling regimes

Yuma Okazaki,[1,2,*] Satoshi Sasaki,[1,2] and Koji Muraki[1]

[1]*NTT Basic Research Laboratories, NTT Corporation, 3-1 Morinosato-Wakamiya, Atsugi, Kanagawa 243-0198, Japan*
[2]*Department of Physics, Tohoku University, Sendai, Miyagi 980-8578, Japan*

We report shot noise spectroscopy on a semiconductor quantum dot in a cotunneling regime. The dc conductance measurements show clear signatures of both elastic and inelastic cotunneling transport inside a Coulomb diamond. We observed Poissonian shot noise with the Fano factor $F \approx 1$ in the elastic cotunneling regime, and super-Poissonian Fano factor $1 < F < 3$ in the inelastic cotunneling regime. The differences in the value of the Fano factor between elastic and inelastic processes reveal the microscopic mechanisms involved in the cotunneling transport.

Shot noise is a time-dependent current fluctuation reflecting the discreteness of charge carriers.[1] Measurements of shot noise can reveal dynamical mechanisms involved in charge transport. For a conductor in which successive electron tunneling events can be regarded as noninteracting and uncorrelated, the low-frequency Fourier power spectral density S of time-domain current fluctuation is proportional to the time-averaged current I, expressed as $S = 2eI$ with e being the charge of the carrier. This type of noise is called Poissonian shot noise. For general conductors, the value of S can be either enhanced or suppressed with respect to the case of Poissonian noise due to the presence of electron-electron interactions or correlations. To characterize the shot noise properties of various conductors, the Fano factor F, defined as $S = 2eFI$, is generally used. $F < 1$ ($F > 1$) characterizes shot noise suppressed (enhanced) with respect to the Poissonian noise, which is referred to as sub-Poissonian (super-Poissonian) noise.

Transport through quantum dot (QD) structures is influenced by electron-electron interactions and correlations, as manifested by the Coulomb blockade[2] and the Kondo effect.[3–5] The interactions and correlations underlying these phenomena alter not only the time-averaged net transport but also the shot noise properties, resulting in both sub-Poissonian and super-Poissonian noise in the Coulomb-blockade and Kondo regimes, respectively.[6–21] Electron cotunneling, one of the fundamental transport mechanisms in QD systems, is a higher order tunneling process which allows a small current to flow in the Coulomb blockade regime.[22–24] Cotunneling is classified into elastic and inelastic processes; the former involves only the QD ground state, while the latter accompanies dynamical charge fluctuation between the ground and excited states. Shot noise measurements in cotunneling regimes enable us to investigate nonequilibrium transport beyond the framework of the linear response theory[13–18] and to elucidate higher order two-electron correlations, including entanglement and nonlocality.[19,20] Previous theoretical investigations have predicted a wide variety of noise behavior in the cotunneling regime; on the other hand, experimental study is still in its infancy.

Onac *et al.*[21] have reported shot noise measurements on a carbon-nanotube QD. Exploiting an on-chip noise detector based on photon-assisted tunneling in a superconducting junction, they observed super-Poissonian noise in the inelastic cotunneling regime. However, in the elastic cotunneling regime below the threshold to the inelastic cotunneling, the current level was too low (<150 pA) for the shot noise to be resolved by their on-chip noise detection scheme. For semiconductor QDs, shot noise measurements in the Coulomb blockade regime are made more challenging by the even lower cotunneling current inherent to semiconductor QDs.[22–24] Gustavsson *et al.*[25] have reported shot noise measurements on a semiconductor QD using a time-resolved charge counting technique, which is capable of resolving the motion of a single electron. Although they have succeeded in extracting the shot noise of the current in the cotunneling regime, no signal associated with either elastic or inelastic cotunneling was detected, because of the limited time resolution of their measurements.

In this paper, we study the shot noise in a semiconductor QD in the Coulomb blockade regime. We employ a direct current noise measurement scheme that exploits a cold amplifier and Fourier-transform-based spectral analysis. In order to facilitate the shot noise measurement in the Coulomb blockade regime, we fabricated a small QD, in which the level spacing ΔE can be increased up to 1 meV. This large ΔE allows us to apply a large source-drain bias voltage and yield a purely elastic cotunneling current of several 100 pA, which is high enough as compared to the resolution of our noise measurement setup utilizing a cold amplifier. Simultaneous dc conductance measurements show clear signatures of both elastic and inelastic cotunneling inside a Coulomb diamond. In the elastic cotunneling regime below the inelastic cotunneling threshold, the measured shot noise shows Poissonian Fano factor $F \approx 1$. In the inelastic cotunneling regime, in contrast, the shot noise is characterized by a super-Poissonian Fano factor $1 < F < 3$, indicating that the inelastic mechanism involves subsequent sequential tunneling processes. Our results, which agree with the theoretically predicted behavior,[17] demonstrate that shot noise spectroscopy can elucidate the microscopic mechanisms involved in the tunneling processes that are indistinguishable in dc transport.

Figure 1(a) shows a scanning electron microscope image of our device and the setup for measuring the current noise. A
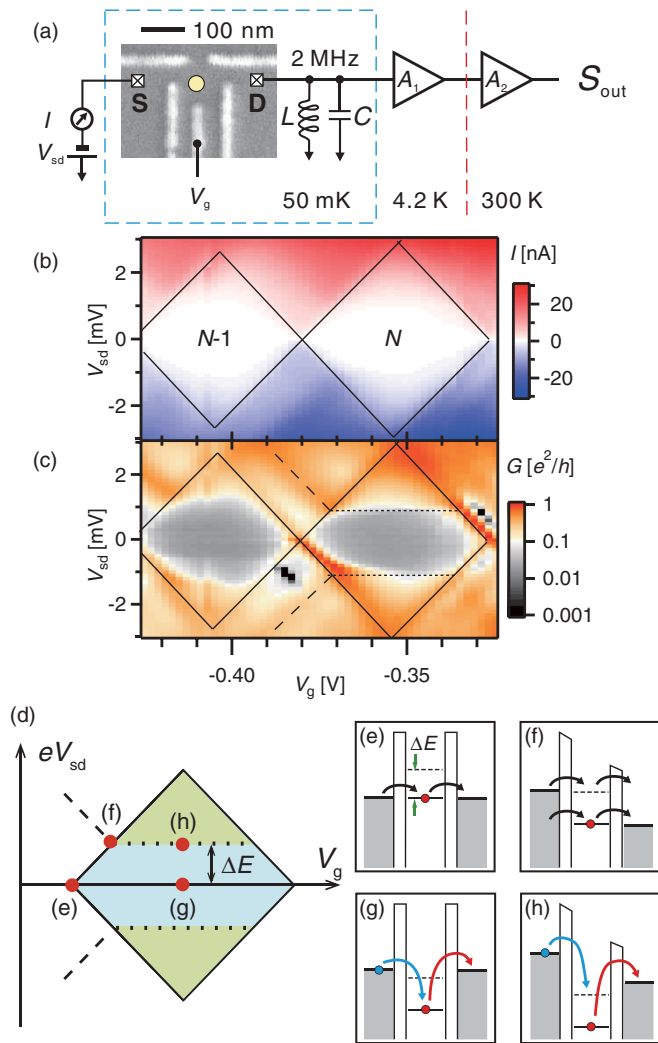
(a)

(b)

(c)

(d)

FIG. 1. (Color online) (a) Scanning electron microscope image of the device and the setup for measuring the current noise. (b) and (c): Color plots of (b) current I and (c) differential conductance G of the QD as a function of V_{sd} and V_g. The solid lines depict the edges of the Coulomb diamond associated with the $(N-1)$- and N-electron valleys. The dashed lines outside the diamond show the onset for the sequential tunneling through the excited state. The dotted lines inside the diamond show the threshold voltage for the inelastic cotunneling. (d)–(h) Schematic illustrations of (d) typical Coulomb diamond structure and [(e)–(h)] tunneling processes relevant in each region shown in (d); (e) sequential tunneling through ground state, (f) sequential tunneling through both ground and excited states, (g) elastic cotunneling, and (h) inelastic cotunneling.

single QD is defined in a shallow two-dimensional electron gas (density $n = 6.7 \times 10^{11}$ cm^{-2} and mobility $\mu = 4 \times 10^5$ cm^2/V s) confined to an Al$_{0.3}$Ga$_{0.7}$As/GaAs/Al$_{0.3}$Ga$_{0.7}$As quantum well of 20 nm width, whose center is located 50 nm below the surface. A QD is formed inside the square area enclosed by the gates, which is 100×100 nm^2 in lithographic dimension. The transport measurements are carried out in a ^{3}He-^{4}He dilution refrigerator with the base temperature $T_b = 50$ mK. The gate voltage V_g is applied to the center gate in order to control the charge states in the QD. A source-drain bias voltage V_{sd} is applied to the source contact (S), while

the drain contact (D) is shunted to the cold ground through the inductor L. The resulting dc current I is measured at the source side. Additionally, the differential conductance $G = dI/dV_{sd}$ is simultaneously measured using a standard lock-in technique with 2-μV ac excitation at 23 Hz.

To measure current noise with higher resolution, we employ a direct current noise measurement scheme that utilizes a cold amplifier and Fourier-transform-based spectral analysis.[26–28] In our setup, the current noise from the QD, with its power spectrum density S_{QD}, is fed to an LC tank circuit with a center frequency of $\approx$2 MHz. At this frequency, $1/f$ noise is negligible and so only shot noise and thermal noise contribute to the measured S_{QD}. Our system was calibrated using the thermal noise measured for various resistances at 12 different temperatures from 200 to 700 mK. The resolution in the current noise is $\delta S \approx 2 \times 10^{-29}$ A^2/Hz, which corresponds to a Poissonian noise of 60 pA.[30]

Figure 1(b) depicts the current through the QD as a function of V_g and V_{sd}. The current is suppressed in the two adjacent diamonds indicated by the solid lines. Inside each diamond, the first-order electron tunneling is energetically prohibited (the Coulomb blockade[2]), and the QD has a well-defined number of electrons denoted by N and $N - 1$. Note that N here is even, because the $N + 1$ valley exhibits the Kondo effect[4] when the dot-lead coupling is slightly increased (data not shown).

Figure 1(d) illustrates a typical Coulomb diamond structure and the tunneling processes relevant to each region. Outside the diamond, sequential tunneling allows a current flow through single-particle levels in the QD [Figs. 1(e) and 1(f)]. Inside the diamond, transport through the QD is allowed only via a higher order tunneling process, the so-called "cotunneling," in which tunneling of an electron from the source to the blockaded QD occurs simultaneously with tunneling of another electron from the QD to the drain through a virtual state. Elastic cotunneling conserves the energy of the QD system before and after the process, leaving the QD in the ground state [Fig. 1(g)]. In contrast, inelastic cotunneling, which leaves the QD in an excited state [Fig. 1(h)], requires an energy supplied from the source-drain bias voltage.[22–24] Accordingly, inelastic cotunneling is allowed only for source-drain biases above a certain threshold eV_{sd}, which is equal to the level spacing ΔE and is therefore independent of V_g [Fig. 1(d)].

Measuring the differential conductance as a function of V_g and V_{sd} reveals additional structures inside the N-electron diamond [Fig. 1(c)], which are associated with cotunneling processes. The horizontal steps at $|V_{sd}| \approx 1$ meV, above which the conductance is strongly enhanced, represent the onset of inelastic cotunneling. From the inelastic cotunneling thresholds, the energy difference between the ground and first excited states of the N-electron diamond is deduced to be $\Delta E = 1$ meV. Below the thresholds ($|eV_{sd}| < \Delta E$), we observe a small but finite conductance $G \approx 0.02$ e^2/h, indicating the elastic contribution [see also Fig. 3(e)]. As we show below, the large energy splitting ΔE in our QD is essential for the observation of shot noise associated with the elastic cotunneling process. These dc transport measurements also allow us to deduce other device parameters: The on-site Coulomb interaction $U = 2$ meV is deduced from the width (3 meV) of the N-electron diamond (which equals $U + \Delta E$), and the dot-lead coupling strength $\Gamma = 0.4$ meV from the
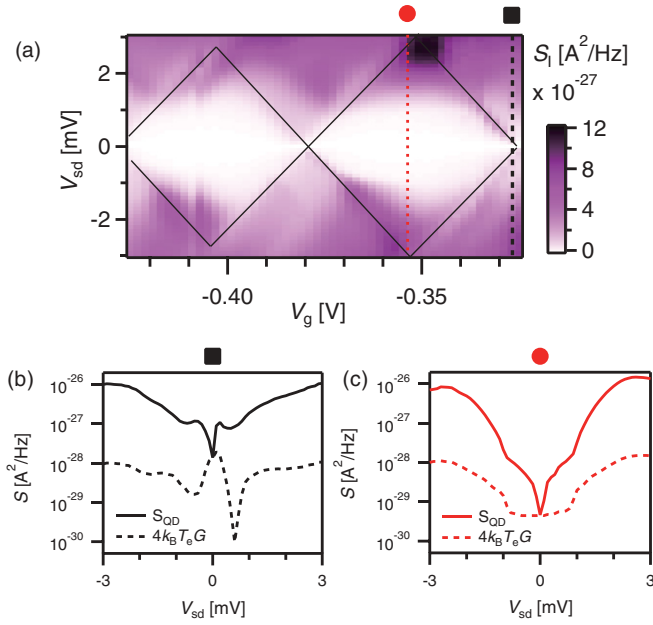
FIG. 2. (Color online) (a) Color plot of the shot noise S_I as a function of V_{sd} and V_g. (b) [(c)] Total current noise $S_{QD}(V_{sd})$ and the estimated thermal noise $4k_B T_e G(V_{sd})$ with the base electron temperature $T_e = 90$ mK at $V_g = -0.327$ V ($V_g = -0.353$ V) square (circle) in (a).

width of the Coulomb peak. We estimated the number of electrons in the QD to be $N \sim 10$ from the effective diameter of the QD (~ 40 nm).

Shot noise $S_I(V_{sd})$ is obtained as a function of V_{sd} by subtracting the thermal noise from the total current noise $S_{QD}(V_{sd})$ measured at each V_{sd}; i.e., $S_I(V_{sd}) = S_{QD}(V_{sd}) - 4k_B T_e G(V_{sd})$. Here, the thermal noise is calculated from the electron temperature T_e and the measured $G(V_{sd})$. We estimate $T_e \approx 90$ mK via the relation $S_{QD}(0) = 4k_B T_e G(0)$, which is expected to hold because $S_I(0) = 0$. The obtained S_I is shown in Fig. 2(a) for the same range of V_g and V_{sd} as in Figs. 1(b) and 1(c). We find that S_I and G [Fig. 1(c)] show qualitatively similar behavior as a function of V_g and V_{sd}.

In the above analysis, we assumed that T_e was constant and independent of V_{sd}. However, it is possible that for large $|V_{sd}|$ the high current induces electron heating and enhances the thermal noise above the expected value, which would result in the overestimation of S_I. To examine the validity of our analysis, in Figs. 2(b) and 2(c), we compare the measured noise and the thermal noise estimated with $T_e = 90$ mK (constant) for two representative cases: (b) the sequential tunneling regime ($V_g = -0.327$ V) and (c) the cotunneling regime ($V_g = -0.353$ V). In both cases, the estimated thermal noise is about two orders of magnitude smaller than the measured noise in the relevant range, $|V_{sd}| > 1$ mV. This guarantees that the above analysis remains valid unless extremely strong heating leads to $T_e \gg 1$ K. As we see below, the negligible contribution of the heating effect can also be confirmed by the Fano factor in the sequential tunneling regime. Even with the current as high as $I > 20$ nA at $V_{sd} = 3$ mV, the measured Fano factor is within the expected range, $F < 1$ [Fig. 3(d)], indicating that the current-induced excess thermal noise is negligible compared with the shot noise.
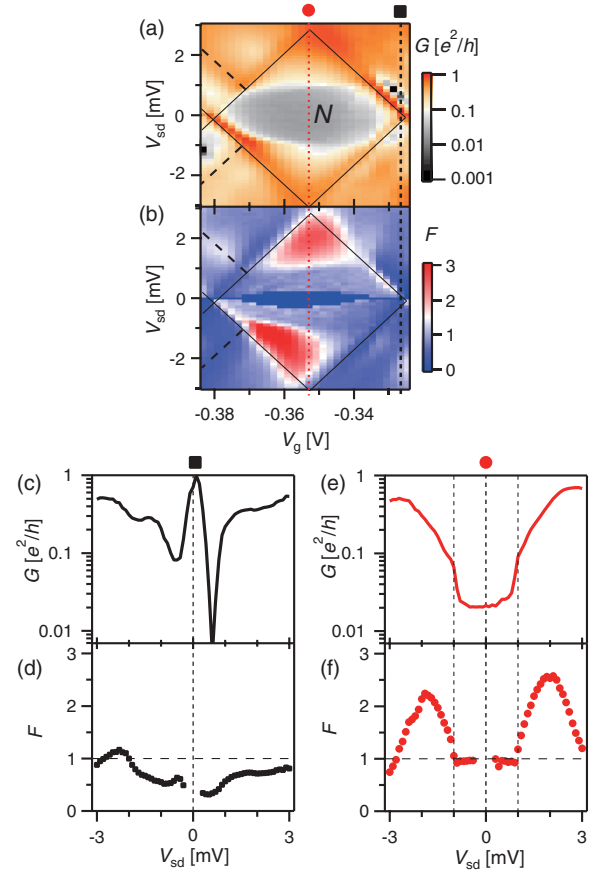

FIG. 3. (Color online) (a) and (b): Color plots of (a) differential conductance G and (b) Fano factor $F = S_I/2eI$ for the N-electron diamond as a function of V_{sd} and V_g. We set $F = 0$ in the region close to $V_{sd} = 0$, where $I \sim 0$ and S_I is below the resolution of our noise measurement system. (c) and (d) [(e) and (f)]: Differential conductance G and Fano factor F traced along the black (red) vertical dotted line in (a) and (b) corresponding to the sequential tunneling (cotunneling) regime. In (d) and (f), Poissonian Fano factor $F = 1$ is shown as horizontal dashed lines. The vertical dashed lines at $V_{sd} = \pm 1$ mV in (e) and (f) indicate the inelastic cotunneling thresholds.

Below, we mainly focus on the region of N-electron diamond. Several intriguing features become evident when the Fano factor, calculated as $F(V_g, V_{sd}) = S_I(V_g, V_{sd})/2eI(V_g, V_{sd})$, is plotted as a function of V_g and V_{sd} [Fig. 3(b)]. For comparison, the corresponding values of the differential conductance G are shown in Fig. 3(a). In order to highlight the contrasting behavior of shot noise in different transport regimes, in Figs. 3(c)–3(f) we plot the measured conductance G and Fano factor F traced along the black and red vertical dotted lines in Figs. 3(a) and 3(b). First, a clear suppression of shot noise is observed in the sequential tunneling regime outside the Coulomb diamond, where the Fano factor varies between $0.5 < F < 1$ as a function of V_{sd} [Fig. 3(d)]. This sub-Poissonian noise for the sequential tunneling regime agrees with the reported value.[6,12] Inside the diamond, we find Poissonian shot noise $F \approx 1$ (the measured value is $F = 0.95 \pm 0.05$) in the elastic cotunneling regime ($|V_{sd}| < 1$ mV) and super-Poissonian shot noise with the Fano factor $1 < F < 3$ in the inelastic cotunneling regime ($|V_{sd}| > 1$ mV) [Fig. 3(f)]. It is noteworthy that the shot
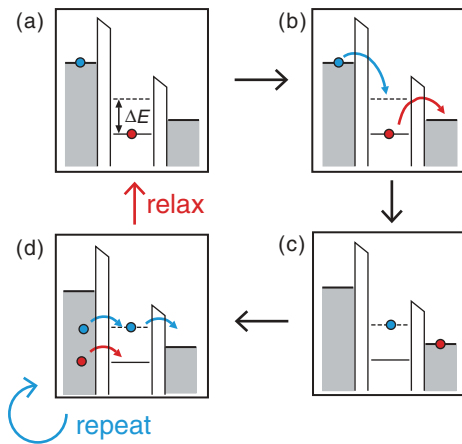
FIG. 4. (Color online) Schematic illustrations of inelastic co-tunneling and subsequent sequential tunneling events that lead to super-Poissonian shot noise.

noise property can clearly distinguish the different transport dynamics in the sequential tunneling and inelastic cotunneling regimes, which is not apparent from the values of G [Figs. 3(c) and 3(e)].

We now discuss in more detail the shot noise properties in the cotunneling regime [Fig. 3(f)]. In the case of elastic cotunneling, the system returns to its ground state after each tunneling event.[16,17] This implies that only one electron is transported through each cycle. Accordingly, $F = 1$ is expected when elastic cotunneling is the dominant transport mechanism. Indeed, our observation of Poissonian Fano factor $F \approx 1$ for $|V_{sd}| < 1$ mV agrees well with this expectation, demonstrating that the transport is dominated by elastic cotunneling in this regime. In turn, the super-Poissonian Fano factor $1 < F < 3$ observed in the inelastic cotunneling regime ($|V_{sd}| > 1$ mV) implies that the transport occurs through a bunched flow of electrons involving on average F electrons. This Fano-factor enhancement can be understood by noting

that inelastic cotunneling leaves the QD in the excited state, and so it must be followed by relaxation processes before the system returns to its original state [Figs. 4(a)–4(c)]. The possible energy relaxation processes include acoustic-phonon emission[29] and sequential tunneling.[17,18,21] In the former, however, only one electron is emitted through each cycle. In contrast, if inelastic cotunneling is followed by a subsequent sequential tunneling process, it happens that more than one electron is transported in each cycle before the system returns to the original state [Fig. 4(d)]. Note that the sequential tunneling process through the excited state can occur repeatedly several times until the system eventually relaxes to the ground state ("repeat" in the Fig. 4). The Fano factor is thus enhanced, reflecting the number of repetitions of this sequential tunneling process. The observed value of $F \sim 2.5$ indicates that the subsequent sequential tunneling process is repeated on average 1.5 times, if relaxation via phonon emission is negligible. For even larger V_{sd} such that the transport window involves the single-particle levels in the QD, the Fano factor is expected to be suppressed to the sub-Poissonian value, since the sequential tunneling becomes dominant. Indeed, in Fig. 3(f), the Fano factor is gradually suppressed to sub-Poissonian noise for $|V_{sd}| > 2$ mV.

In conclusion, we have reported shot noise measurements on a semiconductor quantum dot in the cotunneling regime. The large level spacing ΔE yielded cotunneling current high enough for the shot noise to be resolved in our measurement system. We observed Poissonian shot noise $F \approx 1$ in the elastic cotunneling regime and super-Poissonian shot noise $1 < F < 3$ in the inelastic cotunneling regime. This result demonstrated that shot noise spectroscopy reveals the microscopic mechanisms involved in the cotunneling transport.

*okazaki.y@lab.ntt.co.jp

[1] Ya. M. Blanter and M. Buttiker, Phys. Rep. **336**, 1 (2000).

[2] L. P. Kouwenhoven, C. M. Markus, P. L. McEuen, S. Tarucha, R. M. Westervelt, and N. S. Wingreen, in *Mesoscopic Electron Transport*, edited by L. L. Sohn, L. P. Kouwenhoven, and G. Schön, NATO Advanced Studies Institute, Series E: Applied Science, Vol. 345 (Kluwer, Dordrecht, 1997), p. 105.

[3] D. Goldhaber-Gordon, H. Shtrikman, D. Mahalu, D. Abusch-Magder, U. Meirav, and M. A. Kastner, Nature (London) **391**, 156 (1998).

[4] M. Grobis, I. G. Rau, R. M. Potok, and D. Goldhaber-Gordon, in *Handbook of Magnetism and Advanced Magnetic Materials*, Vol. 5 (Wiley, New York, 2007), pp. 2703–2724.

[5] M. Pustilnik and L. Glazman, J. Phys.: Condens. Matter **16**, R513 (2004).

[6] V. V. Kuznetsov, E. E. Mendez, J. D. Bruno, and J. T. Pham, Phys. Rev. B **58**, R10159 (1998).

[7] E. Sela, Y. Oreg, F. von Oppen, and J. Koch, Phys. Rev. Lett. **97**, 086601 (2006).

[8] A. O. Gogolin and A. Komnik, Phys. Rev. Lett. **97**, 016602 (2006).

[9] A. Golub, Phys. Rev. B **73**, 233310 (2006).

[10] O. Zarchin, M. Zaffalon, M. Heiblum, D. Mahalu, and V. Umansky, Phys. Rev. B **77**, 241303 (2008).

[11] Y. Yamauchi, K. Sekiguchi, K. Chida, T. Arakawa, S. Nakamura, K. Kobayashi, T. Ono, T. Fujii, and R. Sakano, Phys. Rev. Lett. **106**, 176601 (2011).

[12] Yiming Zhang, L. DiCarlo, D. T. McClure, M. Yamamoto, S. Tarucha, C. M. Marcus, M. P. Hanson, and A. C. Gossard, Phys. Rev. Lett. **99**, 036603 (2007).

[13] A. Cottet, W. Belzig, and C. Bruder, Phys. Rev. B **70**, 115315 (2004).

[14] W. Belzig, Phys. Rev. B **71**, 161301(R) (2005).

[15] A. Thielmann, M. H. Hettler, J. König, and G. Schön, Phys. Rev. Lett. **95**, 146806 (2005).

[16] A. Thielmann, M. H. Hettler, J. König, and G. Schön, Phys. Rev. B **71**, 045341 (2005).

[17] I. Weymann, J. Barnaś, and S. Krompiewski, Phys. Rev. B **78**, 035422 (2008).

[18] J. Aghassi, M. H. Hettler, and G. Schön, Appl. Phys. Lett. **92**, 202101 (2008).

[19] D. Loss and E. V. Sukhorukov, Phys. Rev. Lett. **84**, 1035 (2000).

[20] E. V. Sukhorukov, G. Burkard, and D. Loss, Phys. Rev. B **63**, 125315 (2001).

[21] E. Onac, F. Balestro, B. Trauzettel, C. F. J. Lodewijk, and L. P. Kouwenhoven, Phys. Rev. Lett. **96**, 026803 (2006).

[22] S. De Franceschi, S. Sasaki, J. M. Elzerman, W. G. van der Wiel, S. Tarucha, and L. P. Kouwenhoven, Phys. Rev. Lett. **86**, 878 (2001).

[23] D. M. Zumbühl, C. M. Marcus, M. P. Hanson, and A. C. Gossard, Phys. Rev. Lett. **93**, 256801 (2004).

[24] R. Schleser, T. Ihn, E. Ruh, K. Ensslin, M. Tews, D. Pfannkuche, D. C. Driscoll, and A. C. Gossard, Phys. Rev. Lett. **94**, 206805 (2005).

[25] S. Gustavsson, M. Studer, R. Leturcq, T. Ihn, K. Ensslin, D. C. Driscoll, and A. C. Gossard, Phys. Rev. B **78**, 155309 (2008).

[26] R. de-Picciotto, M. Reznikov, M. Heiblum, V. Umansky, G. Bunin, and D. Mahalu, Nature (London) **389**, 162 (1997).

[27] L. DiCarlo, Y. Zhang, D. T. McClure, C. M. Marcus, L. N. Pfeiffer, and K. W. West, Rev. Sci. Instrum. **77**, 073906 (2006).

[28] M. Hashisaka, Y. Yamauchi, S. Nakamura, S. Kasai, K. Kobayashi, and T. Ono, J. Phys.: Conf. Ser. **109**, 012013 (2008).

[29] T. Fujisawa, T. H. Oosterkamp, W. G. van der Wiel, B. W. Broer, R. Aguado, S. Tarucha, and L. P. Kouwenhoven, Science **282**, 932 (1998).

[30] See Supplemental Material at http://link.aps.org/supplemental/10.1103/PhysRevB.87.041302 for more details.